An efficient technique for creating a continuum of equal-area map projections

Daniel "daan" Strebe

View supplementary material ⎘

Published online: 05 Dec 2017.

Submit your article to this journal ⎘

View related articles ⎘

View Crossmark data ⎘

Taylor & Francis
Taylor & Francis Group

ARTICLE

Check for updates

An efficient technique for creating a continuum of equal-area map projections

Daniel "daan" Strebe ⓘD

Mapthematics LLC, Seattle, WA, USA

ABSTRACT
Equivalence (the equal-area property of a map projection) is important to some categories of maps. However, unlike for conformal projections, completely general techniques have not been developed for creating new, computationally reasonable equal-area projections. The literature describes many specific equal-area projections and a few equal-area projections that are more or less configurable, but flexibility is still sparse. This work develops a tractable technique for generating a continuum of equal-area projections between two chosen equal-area projections. The technique gives map projection designers unlimited choice in tailoring the projection to the need. The technique is particularly suited to maps that dynamically adapt optimally to changing scale and region of interest, such as required for online maps.

1. Introduction

The increasing use of interactive, adaptable maps, particularly in software hosted on the World Wide Web, often begs for seamless transitions between map projections. Compare, for example, the adaptive projection system devised by Jenny (2012) or the National Geographic animation created by Strebe, Gamache, Vessels, and Tóth (2012). Strebe (2016) developed an equal-area, continuous hybrid between Bonne and Albers projections for dynamic or animated maps as a solution to a particular case.

If the adaptable map does not need to preserve areas, then hybridization can be simple, such as a linear combination of the initial and the terminal projections. However, even that simplicity can be deceptive. If the two projections diverge sufficiently in planar topology, then linear combinations could result in unacceptable behavior such as the intermediate projection overlapping itself. An overlap means that two or more points from the sphere map to the same point on the plane, and this happens across a region. See, for example, the "wild vines" Snyder (1985, p. 86) describes for his GS50 projection outside its useful domain.

When the initial and terminal projections (hereafter, the *limiting projections*) are equal-area, and area must be preserved throughout intermediate projections, solutions are much more difficult. This is because linear combinations of equal-area projections do not,

themselves, preserve area in the general case, as shown below. Therefore, efforts to create such transitional projections tended to be bespoke because general techniques for hybridizing equal-area projections had not been developed. Some efforts likely never came to fruition because the hybridization proved intractable.

To hybridize two equal-area projections, we would like to do something like

$$C = kB + (1 - k)A$$

where k is a parametric constant such that $0 \leq k \leq 1$, A is the desired initial projection, B is the desired terminal projection, and C is the resulting hybrid. This would yield a smooth transition from A to B. A continuum of maps between two projections via a parameter in the range [0, 1] is called a homotopy in algebraic topology and related fields.

However, usually the hybrid projection C would not preserve areas. This is demonstrated next. For a spherical projection, the property of equivalence is detected by the following analog to the Cauchy–Riemann equations (Snyder, 1987, p. 28):

$$\frac{\partial y}{\partial \varphi}\frac{\partial x}{\partial \lambda} - \frac{\partial y}{\partial \lambda}\frac{\partial x}{\partial \varphi} = s \cos \varphi$$

where s is constant throughout the map, φ is the latitude, and λ is the longitude. Equivalence can be defined strictly or loosely; Snyder's definition is strict in that $s = R^2$ only, where R is the radius of the globe.

By this definition, any region on the globe has the same area on the map. By a looser definition, s may be any finite, nonzero value. The rationale in the looser case is that all regions on the map remain proportioned correctly to each other. The looser definition permits an affine transformation, as any constant, nondegenerate, 2×2 real-valued matrix M, to be applied to the Cartesian coordinates of an equal-area mapped function, resulting in a new equal-area projection. In this case $s = R^2 / \det(M)$. When s is not relevant, we assume $s = 1$ for a unit sphere and identity linear transformation, giving:

$$\frac{\partial y}{\partial \varphi}\frac{\partial x}{\partial \lambda} - \frac{\partial y}{\partial \lambda}\frac{\partial x}{\partial \varphi} = \cos \varphi. \tag{1.1}$$

For $C \to x, y$ as a linear combination of the two projections $A \to x_A, y_A$ and $B \to x_B, y_B$, preserving areas would require that

$$\frac{\partial [ky_B + (1-k)y_A]}{\partial \varphi}\frac{\partial [kx_B + (1-k)x_A]}{\partial \lambda}$$
$$- \frac{\partial [ky_B + (1-k)y_A]}{\partial \lambda}\frac{\partial [kx_B + (1-k)x_A]}{\partial \varphi}$$
$$= \cos \varphi. \tag{1.2}$$

However, simultaneously,

$$\frac{\partial y_A}{\partial \varphi}\frac{\partial x_A}{\partial \lambda} - \frac{\partial y_A}{\partial \lambda}\frac{\partial x_A}{\partial \varphi} = \cos \varphi$$
$$\frac{\partial y_B}{\partial \varphi}\frac{\partial x_B}{\partial \lambda} - \frac{\partial y_B}{\partial \lambda}\frac{\partial x_B}{\partial \varphi} = \cos \varphi$$

which, substituting into Equation (1.2), implies

$$\frac{\partial y_B}{\partial \varphi}\frac{\partial x_A}{\partial \lambda} + \frac{\partial y_A}{\partial \varphi}\frac{\partial x_B}{\partial \lambda} - \frac{\partial y_B}{\partial \lambda}\frac{\partial x_A}{\partial \varphi} - \frac{\partial y_A}{\partial \lambda}\frac{\partial x_B}{\partial \varphi}$$
$$= 2\cos \varphi. \tag{1.3}$$

This equality places stringent constraints beyond just equivalence upon choices for A and B. Therefore, linear combinations of arbitrary choices for A and B will not themselves be equivalent.

New equal-area projections can be generated via a variety of simple transformations applied to known equal-area projections. As mentioned above, any non-degenerate, affine transformation to an equal-area projection yields an equal-area projection. Or, all mapped points sharing the same y value can deform into the arc of a circle, with neighboring horizontals becoming concentric arcs. Applied to the sinusoidal projection, this technique results in the Bonne projection. Other methods appear in the literature, such as *Umbeziffern* (renumbering), first used by Hammer to develop the Hammer from the Lambert azimuthal equal-area, and then named and elaborated on by Wagner (1949) for several of his projections. And so on.

More sophisticated new equal-area projections can be created at will because any equal-area projection can become an area-preserving transformation applied to any other equal-area projection, given suitable scaling. This was the basis for the Strebe 1995 projection [Šavrič, Jenny, White, and Strebe (2015)], for example, where Strebe scales the Eckert IV projection to fit within the confines of a Mollweide projection; back-projects the results to the sphere; and then forward projects to the plane via the Hammer. However, results depend on the projections available rather than on specific needs of the projection designer, and also do not obviously contribute to hybridization.

Some techniques for generating new equal-area projections were developed to approximate desirable distortion characteristics. Snyder (1988) gives a transformation that can be applied to Lambert azimuthal equal-area and repeatedly thereafter in order to coax the angular isocols toward desired paths. Canters (2002) gives polynomial transformations for the same purpose that can be applied to any equal-area map and optimized via, for example, simplex minimization against specified constraints. Neither technique appears obviously adaptable to generating homotopies. Given the amount of calculation involved, neither technique would be well suited to dynamic maps in any case.

2. Background

In describing local distortion on a map projection, the usual metric is Tissot's indicatrix, presented in 1859 by Tissot (1881). The indicatrix projects an infinitesimal circle from the manifold to the plane. On smooth portions of the map, the circle deforms into an ellipse with semimajor axis a and semiminor axis b. If $a \times b$ is constant throughout the indicatrices of the map, then the map is equal-area. If $a = b$ throughout the map, then the map is conformal.

As noted by Laskowski (1989), Tissot's indicatrix of a projected point can be described via the singular value decomposition of the point's column-scaled Jacobian matrix. Hereafter the Jacobian will be denoted J. In the case of a sphere-to-plane projection, the affine transformation representing the complete Tissot ellipse T is given by

$$T = J \cdot \begin{bmatrix} \sec \varphi & 0 \\ 0 & 1 \end{bmatrix}. \tag{2.1}$$

In particular, the areal inflation or deflation (or generically *flation*, as per Battersby, Strebe, and Finn (2016)) can be calculated as

$$s = \det T. \tag{2.2}$$

The term *isocol* appears in Section 1. The term is specific to cartographic maps, and denotes a level curve of distortion. In the case of a conformal map, it is the level curve of constant scale factor. In the case of an equal-area map, it is the level curve of constant angular deformation, which also implies Tissot ellipses of constant dimensions. For maps that are neither conformal nor equal-area, the term is not defined, although isocols of angular deformation and isocols of flation both apply and generally do not coincide.

The term *standard parallel* appears in the text as an attribute of a conic projection. This is the cartographic term for the geographic parallel along which the conic projection is undistorted. Conceptually, it is the circle of tangency of the cone on the sphere. When there are two standard parallels, they are, conceptually, the secant circles – that is, where the cone cuts through the sphere. "Conceptually," because generally the projections involved are not literal perspectives.

3. Development

3.1. Observations

(1) By the loose definition of equal-area transformation, an equal-area projection A from manifold (such as sphere) to plane, then scaled by s, and thence deprojecting back to the manifold via the inverse A' – that is, $A'_s = A'(s \cdot A)$ – results in the area-preserving transformation A'_s from the manifold to itself. This must be true because each step preserves relative areas. In general, the result covers only part of the manifold, and indeed s ought to be chosen such that $s \leq 1$. Hereafter we refer to this parametric s as k such that $[0 \leq k \leq 1]$.

(2) Projecting A'_k to the plane via some other area-preserving transformation B yields an equal-area projection C_k.

(3) Scaling C_k by $1/k$ yields C having the same nominal scale as A: that is, any region in A will have the same area measure in C, insofar as B's area change is unity.

(4) As $k \to 0$, the fraction of projection B's range that is devoted to the transformation shrinks toward a single point, and so C's distortion characteristics approach being described by a single Tissot indicatrix.

(5) If A'_k is contrived such that an "anchor point" P' on the manifold remains undistorted by $A'(k \cdot A)/k$, and contrived such that the Tissot indicatrix at $P = B(P')/k$ shows no distortion,

then C will be merely $k \cdot A$ as $k \to 0$. This is true despite having been projected by B because B has no distortion locally at B and therefore does not contribute to projection.

(6) If k is chosen to be 1, then the deprojection procedure giving A'_k results in full coverage of the original manifold, undistorted, and therefore C will be merely B.

(7) In a "reasonable" projection B, distortion increases away from P in most directions if P has no distortion.

These observations lay the groundwork for the technique. While the observations above, and the technique to follow, are applicable to any sufficiently smooth manifold, the remainder of this monograph discusses the sphere specifically, but without loss of generality.

3.2. Synthesis

Let k represent the weight of B desired in the blended projection, such that $(1 - k)$ shall be the weight of A. By Observations (3) and (5), when $k = 0$, we have $k \cdot A/k = A$. By Observation (6), when $k = 1$, we have B.

For k in $(0, 1)$, when k is small, the contribution of B in the description of C is small. This is because the distortion of B is low in the neighborhood of P and therefore, by Observations (5) and (7), its distinguishing characteristics as a projection are small in that region. Meanwhile, the heavy reduction in A's scale due to small k places all of A into that region of low distortion in B. That leaves A's distortion characteristics to dominate.

Conversely, as k increases, the portion of B's range that A fills increases, and this increases the influence of B's unique characteristics. Simultaneously, A's characteristics diminish because the sphere-to-sphere mapping from Observation (2) places points closer and closer to their original location as k increases.

We thereby have a continuum of equal-area map projections. These features fulfill the requirements for an area-preserving homotopy. The technique is illustrated in Figure 1.

Expressing this synthesis using notation introduced heretofore, and presuming no distortion at $P = B(P')$,

$$C = B(A'[k \cdot A])/k. \tag{3.1}$$

In practice, our choice of anchor point P might vary as k varies, so that when k is 0, P has no distortion, but as k increases, P moves toward some center common to both projections, such as a point of bilateral symmetry. This might be our choice if that common center is
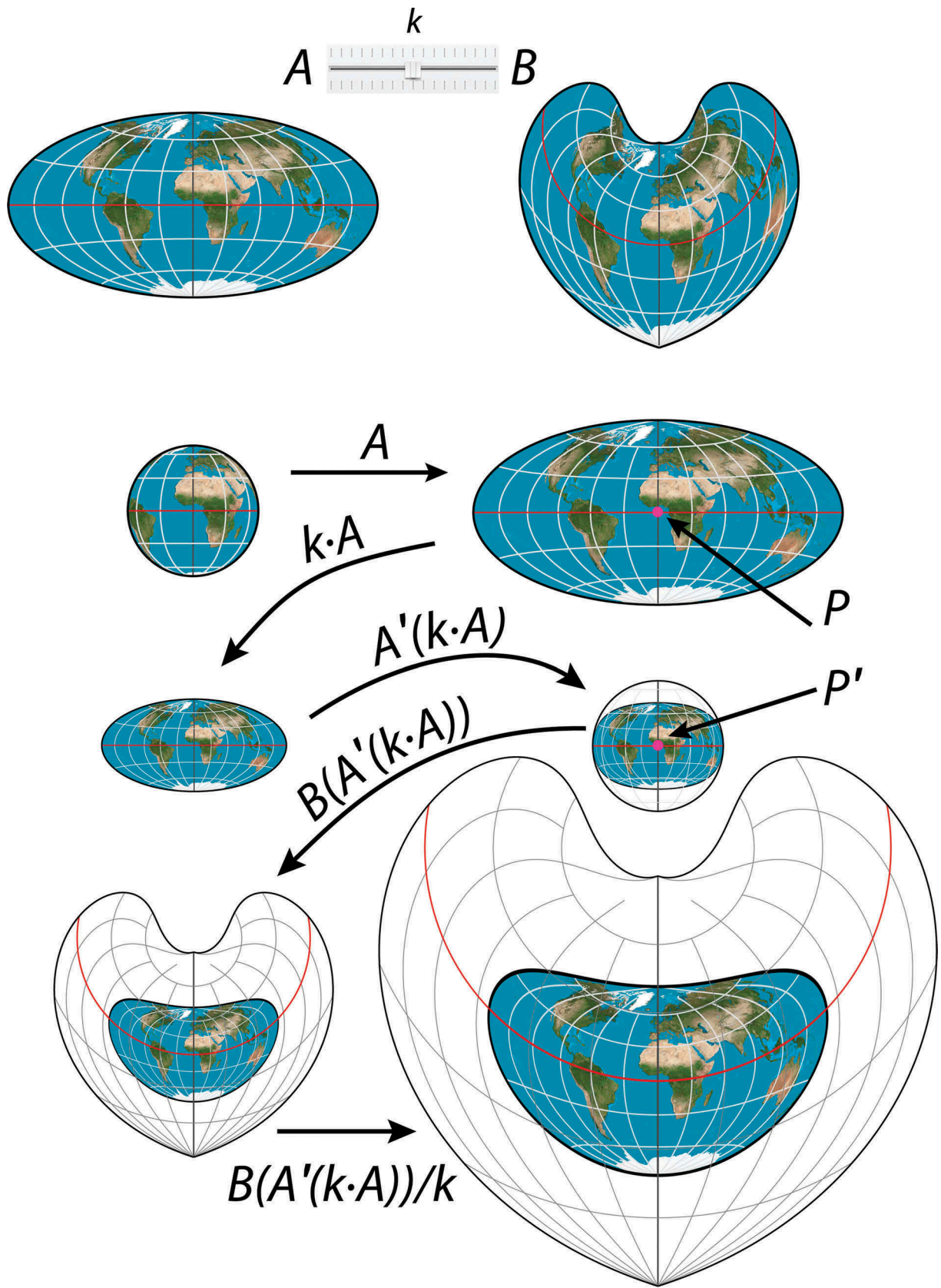
Figure 1. How the homotopy works, $k \approx {}^1/_2$.

distorted in B. Or, perhaps we keep P constant but apply an affine transformation M_B to B for large k in order to eliminate the distortion at the common center P, with M_B approaching identity as $k \to 0$. We express this more general latter case as

$$C = M_B \cdot B(A'[k \cdot A])/k \tag{3.2}$$

where, for example,

$$N_B = k \cdot I + (1 - k) \cdot T_B^{-1}(P)$$
$$M_B = \frac{N_B}{\sqrt{\det N_B}} \tag{3.3}$$

with I as the identity matrix and T_B as given in Equation 2.1 for projection B. This yields a constant determinant of 1 across the parameterization, and therefore preserves area. Obviously other ways of constructing M_B are possible.

Other ways of selecting the anchor point and parameterizing the projections involved might present themselves, depending upon the limiting projections. The example in Appendix Section A.2 demonstrates such a case.

Note a qualification in Observation (5): P' must remain undistorted in A'_k. This is crucial to the technique because the pre-image of $k \cdot A$ has to retain the distortion characteristics of $k \cdot A$ as $k \to 0$. If it does not, then $B(A'_k)/s$ will not result in A as $k \to 0$. Therefore, the scaling by k on the plane must be arranged such that $P = A(P')$ anchors the projection, with the rest shrunk toward it radially. What is important is that P' round-trips to its original position: That is, $P' = A'(k \cdot A[P'])$.

It may be that $A(P')$ does not remain undistorted for the desired P'. For example, if A and B are equatorial pseudocylindric projections, and A is distorted at the center as a vertical elongation, and the desired homotopy would consist of pseudocylindric projections throughout, then more needs to be done. A' yields an undistorted P' because it undoes the distortion A enacted. When then projected by B, if $B(P')$ remains undistorted, then C will be squashed compared to A as $k \to 0$. The stretch could be reintroduced after B. The stretch after B would be linear against k, such that $k = 0$ gives the full compression/stretch, and $k = 1$ gives none. In the general case this can be expressed as

$$C = M_A \cdot M_B \cdot B(A'[k \cdot A])/k \tag{3.4}$$

with M_B as from Equation (3.3) and M_A being the analogous correction for A:

$$N_A = k \cdot I + (1 - k) \cdot T_A(P)$$
$$M_A = \frac{N_A}{\sqrt{\det N_A}}, \tag{3.5}$$

noting that it is not the inverse $T_A^{-1}(P)$ involved, but $T_A(P)$ itself because the goal is to apply the original distortion, not to undo it.

As seen in the examples in Appendix Section A.2, M_A and M_B are not inevitable even when P or P' is distorted, and, in fact, the inverse transformation from $k \cdot A$ back to the sphere need not even use A': *Any equal-area projection that limits to A when $k = 0$ could potentially be used.* M_A and M_B are just general rote devices for reliably achieving a homotopy.

4 Characteristics

4.1. Computational cost

The computational cost of this technique is the cost of A, of A', of B, and a little overhead for scaling and any other adjustments the projection designer might want. Obviously, this is far cheaper than a direct interpretation of the partial derivatives of the projections in play, which would imply computing a double integral for every point. Despite the cheap cost, the result is still superior to the naïve double integral because this technique will not result in overlaps.

4.2. Asymmetry

This technique is sensitive to which of the two chosen projections gets assigned to be A and which to B. That is, the homotopy from A to B differs from the homotopy from B to A. Therefore, the homotopy is directionally asymmetric.

Another asymmetry arises due to the use of linear parameter k as a scale factor in both dimensions when constructing A'_s. A linear progression in k generally yields a weight that favors A. Using $\sqrt{k}$ in place of k throughout the formulations yields a subjectively more linear homotopy.

4.3. Distortion

Distortion characteristics of homotopies between arbitrary pairs of limiting projections are difficult to speak of in generalities. They tend to be highly contingent upon the homotopy. However, if the two limiting projections are chosen such that both have low distortion in the region in which they anchor to each other, we can expect the homotopy to have low distortion throughout the same region. In those cases, regions of unexpected or wildly varying distortion tend to occur only toward the boundary of the hybrid projection, if at all. When boundaries are topologically similar (such as for two pseudocylindric projections), the resulting patterns of distortion can be intuited readily.

4.4. Outer boundary

Projections whose planar topologies are the same retain the common topology under the homotopy. Hence, the continuum between two equatorial pseudocylindric projections with pole-lines, for example, continues to have the outer meridian, duplicated left and right, as its outer boundary, along with a line for the pole. If they have pointed poles, then so will the continuum. If they have flat poles, then so will the continuum. If the initial projection is pointed and the other not, then the continuum will be pointed except at the flat extreme, but the angle of incidence may be imperceptibly slight approaching the flat pole extreme. If the initial projection has a flat pole but the terminal is pointed, then the continuum will be flat throughout, with width shrinking to a point at the terminal extreme.

When the limiting projections' topologies differ, little can be said generally other than that the solution becomes specific to the projections. The description of the boundary is a tractable calculation, but not necessarily simple or convenient. The Lambert azimuthal-to-Albers continuum of Appendix Section A.2 is an example of a nontrivial topological evolution.

4.5. Applicability to conformal and other maps

In cartography, one might need a homotopy between two conformal projections. Due to the fact that any analytic function acting on a conformal map results in another conformal map, a wealth of functions can be drawn upon and composed in order to do this. However, when acting purely on the plane, nothing guarantees a priori that a given mapping will behave well, with the potential for the map failing bijection criteria being an acute concern. While it is common for cartographic maps not to be invertible at singularities or along some boundaries, overlapping of regions is not acceptable for ranges that must be preserved in the mapping. Naïve blending techniques, such as linear combinations of the two projected spaces, hazard such overlapping.

Fortunately, nothing about this homotopy is specific to equal-area projections. As a general topological procedure, it can be used for any sufficiently smooth mapping from any sufficiently smooth manifold. It can be used equally successfully for conformal maps, and indeed, it preserves conformality in the intermediate maps. The only caveat is that the affine transformations M_A and M_B must not contain shear components, but instead only scale isotropically and/or rotate. Since the shear components in M_A and M_B as given in Section 3.2 are present only to correct for non-conformal behavior in equal-area maps, they could have no purpose in a conformal mapping anyway.

Likewise, this homotopy can be developed between aphylactic (neither conformal nor equal-area) projections, with little expectation of preserving identifiable properties other than topological integrity. Or, for example, it can be used to synthesize a progression between some conformal map and some equal-area map. Such a progression has didactic value and, in dynamic maps, perhaps even practical value when the thematic focus of the map changes or when zooming out from large scale to medium and small scales.

5. Conclusion

By combining several observations about equal-area maps in a novel way, this research produced a tractable technique for hybridizing any two equal-area projections. Using such transitions, a map designer might find combinations that yield distortion characteristics more favorable to the region being mapped than are otherwise available. Because of the generality of the technique, and the fact that its parameterization operates on the topology of the sphere (or ellipsoid or other manifold), the technique can hybridize even projections of otherwise incompatible planar topologies, such as an azimuthal and a conic projection. The problem of tailored projections has been acute for equal-area needs, since no simple, general system existed. This new technique fills the void.

The same ability to parameterize for new projections between known projections makes the technique well suited for dynamic mapping and animations. For the first time, equal-area projections can dynamically adapt optimally for the entire region brought into view when panning and zooming.

The technique is computationally cheap (that is, on the order of the limiting projections involved); completely general; and not limited to equal-area maps. Because the technique is built upon the topology of the surface being projected, rather than acting purely in Cartesian space, overlapping can be avoided with minimal precautions, unlike a simple linear combination of the limiting projections. Therefore, the technique applies equally well to conformal projections, projections that are neither conformal nor equal-area, and even hybridizing conformal projections with equal-area projections.

Acknowledgments

Disclosure statement

ORCID

Daniel "daan" Strebe 🔘 http://orcid.org/0000-0001-6410-6259

References

Battersby, S. E., Strebe, D., & Finn, M. P. (2016). Shapes on a plane: Evaluating the impact of projection distortion on spatial binning. *Cartography and Geographic Information Science*, 44, 410–421. doi:10.1080/15230406.2016.1180263

Canters, F. (2002). *Small-scale map projection design*. London: Taylor & Francis.

Jenny, B. (2012). Adaptive composite map projections. *IEEE Transactions on Visualization & Computer Graphics*, 18, 2575–2582. doi:10.1109/TVCG.2012.192

Jenny, B., & Šavrič, B. (2017). Enhancing adaptive composite map projections: Wagner transformation between the lambert azimuthal and the transverse cylindrical equal-area projections. *Cartography and Geographic Information Science.* doi:10.1080/15230406.2017.1379036

Laskowski, P. H. (1989). The traditional and modern look at Tissot's indicatrix. *The American Cartographer*, 16, 123–133. doi:10.1559/152304089783875497

Nell, A. (1890). Äquivalente kartenprojektionen. *Petermanns Mitteilungen*, 36, 93–98.

Šavrič, B., Jenny, B., White, D., & Strebe, D. R. (2015). User preferences for world map projections. *Cartography and Geographic Information Science*, 42, 398–409. doi:10.1080/15230406.2015.1014425

Snyder, J. P. (1985). *Computer-assisted map projection research.* (US Geological Survey Bulletin 1629). Reston, VA: USGS.

Snyder, J. P. (1987). *Map projections – a working manual.* (US Geological Survey Professional Paper 1395). Washington: US Government Printing Office.

Snyder, J. P. (1988). New equal-area map projections for noncircular regions. *The American Cartographer*, 15, 341–356. doi:10.1559/152304088783886784

Strebe, D. (2016). An adaptable equal-area pseudoconic map projection. *Cartography and Geographic Information Science*, 43, 338–345. doi:10.1080/15230406.2015.1088800

Strebe, D., Gamache, M., Vessels, J., & Tóth, T. (2012). Mapping the oceans [video]. *National Geographic Magazine, Digital Edition*, 9. https://www.youtube.com/watch?v=OQCoWAbOKfg

Tissot, N. A. (1881). *Memoire sur la représentation des surfaces et les projections des cartes géographiques*. Paris: Gauthier-Villars.

Wagner, K. (1949). *Kartographische Netzentwürfe*. Leipzig: Bibliographisches Institut.

Appendix. Examples

A.1. Sinusoidal and cylindrical equal-area

The cylindrical equal-area and the sinusoidal projections are two of the simplest equal-area projections from sphere to plane. The cylindrical equal-area projection is defined as

$$\begin{aligned} x &= \lambda \cos \varphi_1 \\ y &= \sec \varphi_1 \sin \varphi \end{aligned} \tag{A1}$$

with φ_1 being the latitude along which scale is correct and conformality preserved. It has Jacobian

$$\begin{bmatrix} \frac{\partial x}{\partial \lambda} = \cos \varphi_1 & \frac{\partial x}{\partial \varphi} = 0 \\ \frac{\partial y}{\partial \lambda} = 0 & \frac{\partial y}{\partial \varphi} = \sec \varphi_1 \cos \varphi \end{bmatrix}. \tag{A2}$$

The projection's inverse is

$$\begin{aligned} \varphi &= \arcsin\left(y \cos \varphi_1\right) \\ \lambda &= x \sec \varphi_1. \end{aligned} \tag{A3}$$

The sinusoidal is defined as

$$\begin{aligned} x &= \lambda \cos \varphi \\ y &= \varphi. \end{aligned} \tag{A4}$$

If we let A be the cylindrical equal-area and B the sinusoidal, then A' is given by the inverse of $k \cdot A$ like so:

$$\begin{aligned} \varphi' &= \arcsin(k \sin \varphi) \\ \lambda' &= k\lambda. \end{aligned} \tag{A5}$$

Notice that φ_1 does not appear in A'; regardless of choice for φ_1, they all result in the same A'. Any A' will undo the distortion enacted by A at P', but in this case, the influence of φ_1 gets removed not only from P' but throughout the projection because the projection parameterized by any φ_1 is just an affine scaling of the same underlying projection. This removal will be counteracted by M_A, computed as

$$N_A = k \cdot I + (1 - k) \cdot T_A(P)$$
$$= \begin{bmatrix} k + (1-k)\cos\varphi_1 & 0 \\ 0 & k + (1-k)\sec\varphi_1 \end{bmatrix}$$

$$M_A = \frac{N_A}{\det N_A} = \begin{bmatrix} \sqrt{\frac{k+(1-k)\cos\varphi_1}{k+(1-k)\sec\varphi_1}} & 0 \\ 0 & \sqrt{\frac{k+(1-k)\sec\varphi_1}{k+(1-k)\cos\varphi_1}} \end{bmatrix}$$

by Equations (2.1), (3.4), and (A2), given $P' = (0°E, 0°N)$. No correction is required for B because sinusoidal has no distortion at P, so $M_B =$

I and can be ignored. $B(A')/k$ is given by applying Equation (A4) to Equation (A5):

$$x = \lambda \sqrt{1 - k^2 \sin^2 \varphi}$$
$$y = \arcsin(k \sin \varphi)/k. \tag{A6}$$

By Equations (3.4) and (A6), then,

$$C = \begin{bmatrix} \sqrt{\frac{k+(1-k)\cos\varphi_1}{k+(1-k)\sec\varphi_1}} & 0 \\ 0 & \sqrt{\frac{k+(1-k)\sec\varphi_1}{k+(1-k)\cos\varphi_1}} \end{bmatrix} \cdot \begin{bmatrix} \lambda\sqrt{1-k^2\sin^2\varphi} \\ \arcsin(k\sin\varphi)/k \end{bmatrix} \tag{A7}$$

and thereby the homotopy from cylindrical equal-area to sinusoidal is

$$x = \lambda\sqrt{1 - k^2\sin^2\varphi}\sqrt{\frac{k+(1-k)\cos\varphi_1}{k+(1-k)\sec\varphi_1}}$$

$$y = \frac{\arcsin(k\sin\varphi)}{k}\sqrt{\frac{k+(1-k)\sec\varphi_1}{k+(1-k)\cos\varphi_1}}. \tag{A8}$$

Parameterized with $k = 0.226$ and $\varphi_1 = 0$ (such that Equation (A6) suffices), this formulation results in a projection that is practically indistinguishable from the pseudocylindric limiting form of the equal-area pseudoconic projection devised by Nell (1890). Nell's is the first known equal-area pseudocylindric with a pole-line, and is a compromise between the sinusoidal and the equal-area cylindric with $\varphi_1 = 0$ (Lambert's). Unlike Nell, no iteration is required in computing Equation (A8), illustrating the technique's characteristic computational efficiency.

To illustrate the asymmetry noted in Section 4.2, we give the reverse homotopy from sinusoidal to cylindrical equal-area, omitting the intermediate calculations:

$$x = \frac{\lambda\cos\varphi\cos\varphi_1}{\cos(k\varphi)}\sqrt{\frac{k+(1-k)\sec\varphi_1}{k+(1-k)\cos\varphi_1}}$$

$$y = \frac{\sin(k\varphi)\sec\varphi_1}{k}\sqrt{\frac{k+(1-k)\cos\varphi_1}{k+(1-k)\sec\varphi_1}}. \tag{A9}$$

This projection is the same as Kavraiskiy's fifth, matching his recommended parameterization at $k = 0.738340936$ and $\varphi_1 = 29.8924267°$.

A.2 Lambert azimuthal equal-area and Albers conic

Albers and Lambert azimuthal equal-area have two highly divergent topologies. The perimeter of Albers is the same as a pseudocylindric projection's: pole lines and the 180th meridian replicated left and right. Lambert, on the other hand, projects the center's antipodal point as a circle of radius 2, given unit sphere. With the constraint that the Lambert be centered on the pole, a homotopy for the two is trivial because Lambert is a limiting form of Albers, with both standard parallels being the pole.

When Lambert needs to be centered elsewhere, however, no obvious solution makes itself known. Jenny (2012) proposed a transformation from Lambert azimuthal to transverse Lambert cylindrical equal-area projection through Albers by using the limiting-form relationship of Lambert to Albers, with other adjustments. However, in order to keep the region of interest away from the split that appears as soon as the homotopy's parameter leaves 0, the Lambert azimuthal must be rotated, pushing the region of interest into higher-distortion portions of the projection. This is not satisfactory because the region of interest is where low distortion is most desired. Jenny and Šavrič (2017) acknowledge this shortcoming and propose an improved transition via a transverse Wagner. However, applicability of the Wagner route is limited to "portrait format" maps. Jenny and Šavrič (2017, p. 6) write:

> A … conic transformation remains in the adaptive composite projection for landscape-format maps for transitioning between the azimuthal (for maps at continental scales) and the conic (for larger scales) projections …. However, distortion caused by the conic transformation is comparatively large …. Improving this transformation between the Lambert azimuthal and the Albers conic projections is an open challenge.

Here we meet this challenge.

The oblique Lambert azimuthal equal-area from the sphere is formulated as

$$z = \sqrt{2}/\sqrt{1 + \sin\varphi_3\sin\varphi + \cos\varphi_3\cos\varphi\cos\lambda}$$
$$x = z\cos\varphi\sin\lambda$$
$$y = z(\cos\varphi_3\sin\varphi - \sin\varphi_3\cos\varphi\cos\lambda) \tag{A10}$$

after Snyder (1987), with its inverse being

$$\rho = \sqrt{x^2 + y^2}$$
$$\varsigma = 2\arcsin\frac{\rho}{2}$$
$$\varphi = \arcsin(\cos c\sin\varphi_3 + y\rho^{-1}\sin c\cos\varphi_3)$$
$$\lambda = \arctan(x\sin c, \rho\cos\varphi_3\cos c - y\sin\varphi_3\sin c) \tag{A11}$$

and arctan being the typical two-argument form yielding the full range $[-\pi, \pi]$. φ_3 is the latitude at which no distortion is wanted, achieved at the central meridian only.

The standard Albers from the sphere is formulated as

$$n = \frac{\sin\varphi_1 + \sin\varphi_2}{2}$$

$$\rho = \frac{\sqrt{\cos^2\varphi_1 + 2n(\sin\varphi_1 - \sin\varphi)}}{n}$$

$$\theta = n\lambda$$
$$x = \rho\sin\theta$$
$$y = -\rho\cos\theta. \tag{A12}$$

Its inverse is not needed here because Albers serves as B, for which only forward is used.

Let Lambert azimuthal equal-area be A and Albers be B. Lambert is undistorted at its point of obliquity $(\varphi_3, 0)$. Albers is undistorted all along selectable constant latitudes φ_1 and φ_2. The angular extent of the Albers wedge is determined by n. Let us assume that $\sin\varphi_3$ is chosen to be n to place it about halfway between the standard parallels. Albers would be distorted at φ_3 – in fact, it reaches a local maximum there – unless $\varphi_1 = \varphi_2 = \varphi_3$. Hence, something must be done for small k so that the area around φ_3 has low distortion then. We could address this by means of M_B as described in Equation (3.2).

Another method presents itself based on the characteristics of Albers. We are free to vary the standard parallels insofar as the sum of their sines is constant so that we do not vary the angular extent of the cone. Hence, if we start at $k = 0$ with $\varphi_{1k} = \varphi_{2k} = \varphi_3$, and gradually move φ_{1k} and φ_{2k} apart as $k \to 1$, we achieve the needed effect. So,

$$\sin\varphi_{1k} = \sin\varphi_1 + (1-k)(\sin\varphi_3 - \sin\varphi_1)$$
$$\sin\varphi_{2k} = \sin\varphi_2 + (1-k)(\sin\varphi_3 - \sin\varphi_2).$$

This frees us to use the simplest form of the transformation. Given A as Equation (A10), A' as Equation (A11), and B as Equation (A12), the homotopy follows immediately from Equation (3.1). The configurable parameters φ_1 and φ_2 are taken as φ_{1k} and φ_{2k} for each k. Delineated, using definitions from Equations (A10) and (A12) unless replaced here:

$$x_L = kz\cos\varphi\sin\lambda$$
$$y_L = kz(\cos\varphi_3\sin\varphi - \sin\varphi_3\cos\varphi\cos\lambda)$$
$$\rho_L = \sqrt{x_L^2 + y_L^2}$$
$$c_L = 2\arcsin\frac{\rho_L}{2}$$
$$\varphi_L = \arcsin(\cos c_L\sin\varphi_3 + y_L\rho_L^{-1}\sin c_L\cos\varphi_3)$$
$$\lambda_L = \arctan(x_L\sin c_L, \rho_L\cos\varphi_3\cos c_L - y_L\sin\varphi_3\sin c_L)$$
$$\rho_A = \sqrt{\cos^2\varphi_{1k} + 2n(\sin\varphi_{1k} - \sin\varphi_L)}$$
$$\theta = n\lambda_L$$
$$x = \frac{\rho_A\sin\theta}{k}$$
$$y = \frac{-\rho_A\cos\theta}{k}. \tag{A13}$$

The results are as shown in Figure 2, with distortion diagrams as Figure 3. We do not address the matter of the perimeter here; its description is complicated and not instructive for other homotopies. Most practical uses of this particular homotopy would bound the region well short of the topological perimeter by some easily described means such as a rectangle or as north/west/south/east extents, mapped.

In a reverse homotopy going from Albers to Lambert, we might again choose to situate P about halfway between the two standard parallels so that we converge most directly from Albers to Lambert azimuthal. To achieve that, we could use M_A as described in Equation
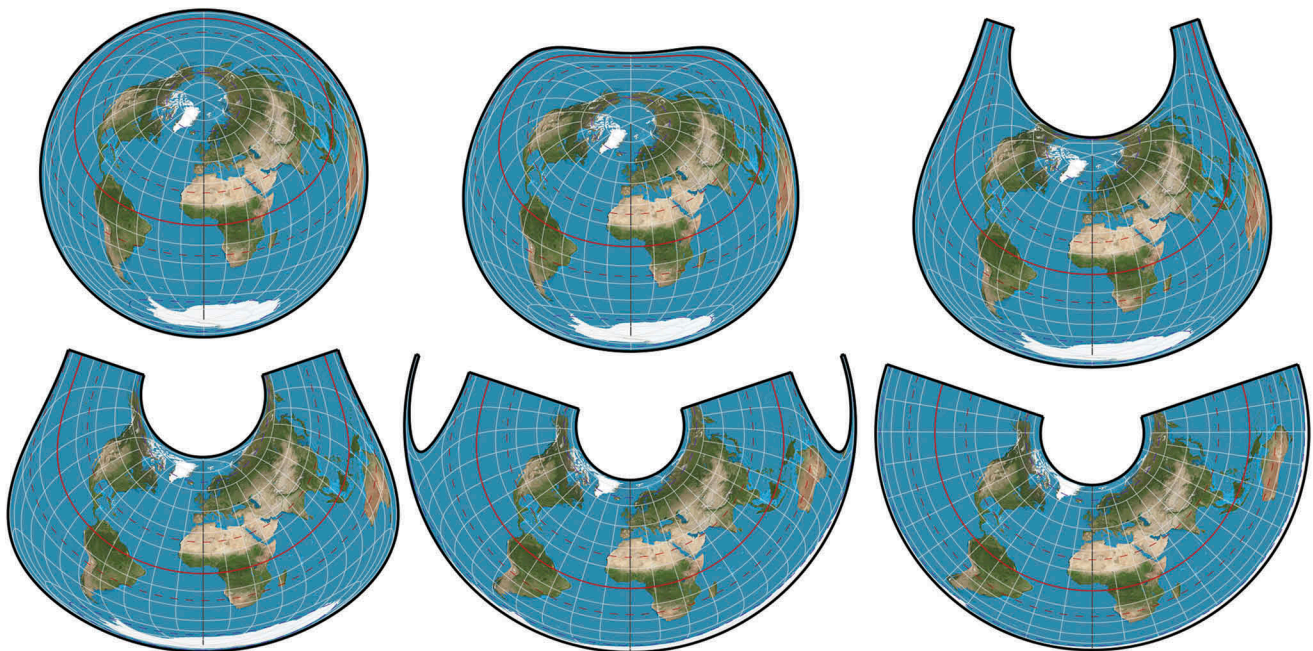

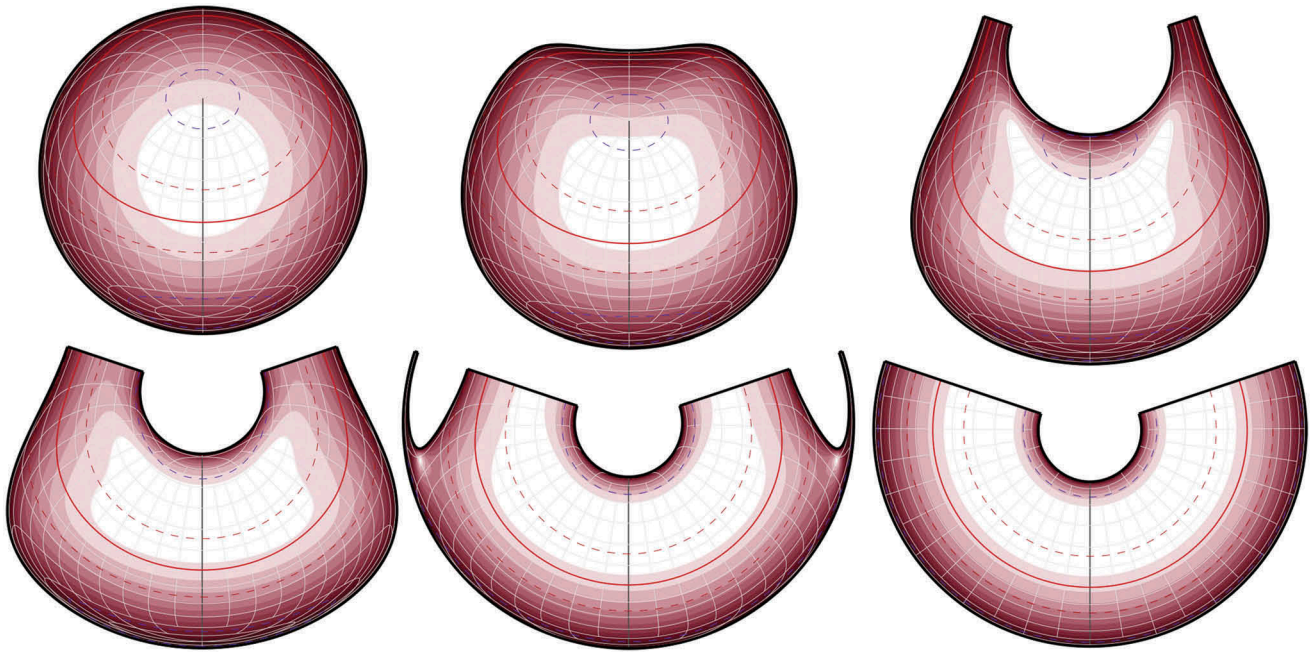**Figure 2.** Homotopy from Lambert azimuthal equal-area to Albers, $\sqrt{k}$ in 0.2 increments.

Figure 3. Patterns of maximum angular deformation, 10° increments, deeper color signifying greater distortion.

(3.2). This would correct for the fact that P reaches a local maximum of distortion on the Albers, whereas if left uncorrected, P would be the point of no distortion and the standard parallels would gain distortion.

However, just as in the forward homotopy, a better method suggests itself. Ideally, we would want the benefits of Albers to dominate for small k. The benefit of Albers is in the two standard parallels having no distortion. We can protract those benefits beyond the vicinity of $k = 0$, at least on the Albers side of the transformation. We can do this by using a different Albers parameterization for the inverse, one whose forward we will call $\hat{A}$. Its parameterization is contrived so that $\hat{A}$ has standard parallels that coincide in Cartesian space with the standard parallels of $k \cdot A$. (See Figure 4.) This works because as $k \to 0$, $\hat{A} \to A$. Because the paths of no distortion on $\hat{A}$ coincide with those on $k \cdot A$, no correctional affine transformation is needed and the homotopy retains more "Albers-ness" over the low parametric space as compared to a rote approach using M_A.

Without getting into computational details, the result of this method from Albers to Lambert, and the round-trip return via Equation (A13), can be seen in the video "Albers-Lambert azimuthal round-trip homotopy" in the Supplementary Material. The corresponding animation showing distortion can be seen in the video "Albers-
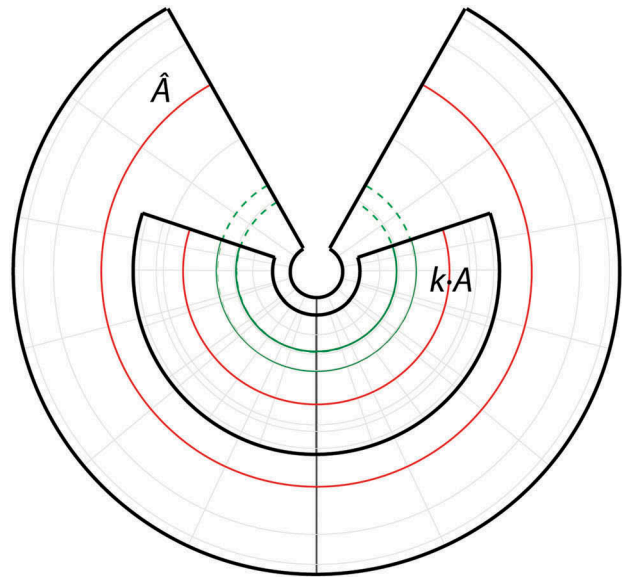

Figure 4. $\hat{A}$ with standard parallels (green dashes) coincident to those of $k \cdot A$ (solid green).

Lambert azimuthal round-trip homotopy distortion" in the Supplementary Material. Lower-quality versions can also be found at https://youtu.be/D1CuUPi2yA0 and https://youtu.be/AcTFAXPLReE.